

## Study of a water desalination station using the SMCEC technique: dynamic modelling and simulation

Habib Ben Bacha<sup>a,b\*</sup>, Tarak Damak<sup>a</sup>, Mounir Bouzguenda<sup>a</sup>,  
Aref Younes Maalej<sup>a,b</sup>, Hamed Ben Dhia<sup>b</sup>

<sup>a</sup>Laboratoire des Systèmes Electro-Mécaniques, <sup>b</sup>Laboratoire de l'Eau de l'Energie et de l'Environnement,  
Department of Mechanical Engineering, Ecole Nationale d'Ingénieurs de Sfax, BP W3038, Sfax, Tunisia  
Tel. +216 (4) 274088; Fax +216 (4) 275595; email: habib.benbacha@enis.rnu.tn

Received 14 July 2000; accepted 28 July 2000

---

### Abstract

The dynamic modelling and simulation of the three sections of a water desalination facility using the Solar Multiple Condensation Evaporation Cycle (SMCEC) technique are presented. The models are obtained using thermal energy and mass balances of the different sections of the unit. The resulting distributed parametric systems of equations are transformed into a system of ordinary differential equations using the orthogonal collocation method. The parametric study in the dynamic mode and the numerical simulation allow to predict the behaviour of output of each of the three unit sections following variations in the internal signals and external perturbations.

*Keywords:* Water desalination; SMCEC; Dynamic modelling; Distributed parameters; Orthogonal collocation; Numerical simulation

---

### 1. Introduction

The SMCEC-based water desalination unit consists of three sections: the solar collectors, the evaporation tower and the condensation tower as shown in Fig. 1. Their description and operation of each section are found in [1,2].

Brackish or seawater heated in the solar collectors is pulverised in the evaporation chamber. Saturated humid air is transported to the condensation tower by either forced or natural convection where it condenses once it is in contact with the condenser cold plates.

---

\*Corresponding author.

*Presented at the conference on Desalination Strategies in South Mediterranean Countries, Cooperation between Mediterranean Countries of Europe and the Southern Rim of the Mediterranean, sponsored by the European Desalination Society and Ecole Nationale d'Ingénieurs de Tunis, September 11–13, 2000, Jerba, Tunisia.*

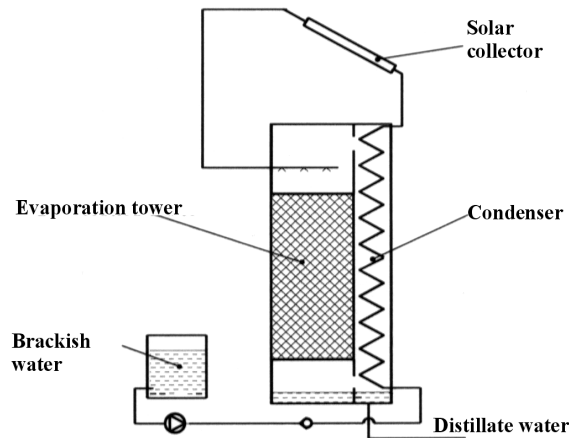


Fig. 1. SMCEC water desalination unit.

Due to the fact that the desalination unit is a multivariable process with many input and output signals and that most of the input signals are external perturbations related to weather conditions, it is first necessary to study and predict the behaviour of the installation following variations in both internal and external signals, and second to study each of the three unit sections separately.

In Section 2 the dynamic model of each stage is developed using thermal energy and mass balances. The obtained models are systems with distributed parameters described essentially by a set of partial derivative equations. These models allow a good description of the real process and monitoring of the spatial distribution and time evolution of the various parameters. Section 3 is dedicated to the parametric study and the simulation results of the reduced model for each section. The objective of the simulation is to predict the behaviour of each section output signals and the system production following variations in the control signals and changes in meteorological conditions. In the last section, results are discussed followed by recommendations for the unit's best operation and production.

## 2. Model formulation

In the SMCEC-based desalination unit multiple phenomena are involved such as heating, evaporation and condensation all in one system, and many of its variables are time and space dependent. Therefore, the unit dynamic behaviour is best described by several parameters in the form of systems of equations with partial derivatives, with the main objectives being the detailed study and optimization of the unit production and control design.

### 2.1. Solar collector modelling

Fig. 2 displays the external factors that would affect the solar collector such as the solar radiation,  $I(t)$ , and temperature,  $T_a(t)$ , and the collector input signals, namely the fluid debit,  $m_f(t)$ , and temperature,  $T_{fe}(t)$ , as well as the output signal which is the fluid temperature,  $T_{fs}(t)$ . Both  $I(t)$  and  $T_a(t)$  are considered perturbations on the system due to their random behaviour. To obtain the dynamic model, the solar collector is divided into small surfaces,  $dS$ , and studied for a very short period of time,  $dt$ , using energy balance equations for  $dS$  using the three hypotheses listed in [3,4].

The thermal balance of the system formed by the absorber and the fluid for a slice of the collector with a width  $l$ , a length  $dx$ , and a surface  $dS=l \cdot dx$  for a time interval,  $dt$ , gives the following model:

$$\frac{\partial T_f}{\partial t} = \frac{1}{b} \left( -m_f d \frac{\partial T_f}{\partial x} - T_f + f(t) \right) \quad (1)$$

with  $d = [(C_f)/(U_1 l)]$  being the fluid debit coefficient,  $b$  the time characteristic, and  $f(t) = [(BI)/(U_1)] + T_a$  the ambient condition function.

Eq. (1) is an equation with partial derivatives whose solution gives the fluid instantaneous temperature at any point of the collector.

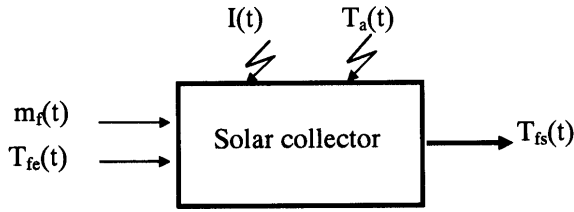


Fig. 2. Input/output block diagram of the solar collector.

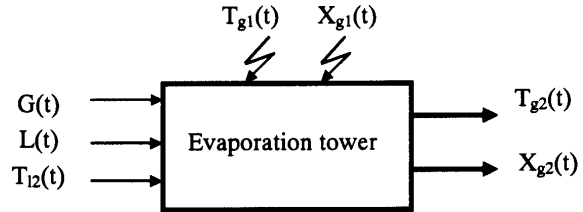


Fig. 3. Input/output block diagram of the evaporation tower.

### 2.2. Evaporation tower modelling

Hot water enters the top of the tower with a debit,  $L(t)$ , and a temperature,  $T_{l2}(t)$ . At the bottom of the tower, incoming air has a debit,  $G(t)$ , a temperature,  $T_{g1}(t)$ , and a water content  $X_{g1}(t)$ . The produced vapour leaves at the top of the tower with a temperature,  $T_{g2}(t)$ , and water content,  $X_{g2}(t)$ . The air circulation mode used in the study is a natural convection with a closed air circuit. The evaporation tower shown in Fig. 3 is a multivariable system with an input signal vector  $[G(t), L(t), T_{l2}(t)]$ , an output signal vector  $[T_{g2}(t), X_{g2}(t)]$  and a perturbation vector  $[T_{g1}(t), X_{g1}(t)]$ . The dynamic model of the evaporation tower is a set of equations with partial derivatives with respect to space and time, developed using thermal and mass balances, taking into account the coupling among water temperature, air temperature and air water content inside the tower. The balance is done on an element of volume with height  $dz$ . The approach is similar to that used in the cooling tower study [4–6]. In order to establish the thermal and mass balances of the tower for the liquid phase, the gas phase, and the liquid–gas interface, the five hypotheses listed in [4–6] are used. Next, the mathematical model for the evaporation tower is developed. It consists of a system of coupled equations with distributed parameters of heat and mass transfers between the hot water coming from the solar collector and the air.

- Water phase:

$$m_1 c_1 \frac{\partial T_1}{\partial t} = LC_1 \frac{\partial T_1}{\partial z} - h_1 a (T_1 - T_I) \quad (2)$$

- Air phase:

$$m_g C_g \frac{\partial T_g}{\partial t} = -GC_g \frac{\partial T_g}{\partial z} + h_g a (T_I - T_g) \quad (3)$$

and

$$m_g \frac{\partial X_g}{\partial t} = -G \frac{\partial X_g}{\partial z} + k_g a (X_I - X_g) \quad (4)$$

and at the air–water interface

$$X_I = X_g + \frac{h_1 (T_1 - T_I) + h_g (T_g - T_I)}{L_v k_g} \quad (5)$$

It can also be expressed as [7–10]:

$$X_I = 0.62198 \frac{P_{ws}}{1 - P_{ws}} \quad (6)$$

where:  $m_1 = \varepsilon_1 \rho_1$ ,  $m_g = \varepsilon_g \rho_g$ , with  $P_{ws}$  being the saturation pressure given by:

$$\ln(P_{ws}) = -6096.938 \frac{1}{T_I} + 21.240964 - 2.711 + 1.67395 \times 10^{-5} T_I^2 + 2.43350 \ln(T_I)$$

The relationships giving the mass exchange coefficients ( $k_g$ ) and the heat exchange coefficients ( $h_1, h_g$ ) as a function of air flow rate ( $G$ ) and water flow rate ( $L$ ) are

$$k_g = \frac{2.09 G^{0.11515} L^{0.45}}{a}$$

and

$$h_1 = \frac{5900 G^{0.5894} L^{0.169}}{a}$$

The air-film heat transfer coefficient and the mass transfer coefficient on the air–water interface are coupled by Lewis relation,  $h_g = C_g k_g$  [5,6].

### 2.3. Condensation tower modelling

At the top of the condensation tower, humid air from the evaporation tower enters with a mass debit,  $G(t)$ , temperature  $T_{g2}(t)$ , and water content  $X_{g2}(t)$ . At the entrance at the bottom of the tower, cold water is injected inside the condensation plates with a debit,  $D_c(t)$ , and temperature,  $T_{c1}(t)$ . At the exit, distillate water is collected from the vapour produced in the evaporation tower with a debit,  $W_c(t)$ , while at the top, preheated water is injected into the solar collector with temperature  $T_{c2}(t)$ . As seen in Fig. 4, the condensation tower can be considered as a multivariable system. In fact,  $[D_c(t), G(t), T_{g2}(t), X_{g2}(t)]$  is the input signal vector,  $[T_{c2}(t), W_c(t)]$  is the output signal vector and  $[T_{c1}(t)]$  is the perturbation vector. Once again, the mathematical model is based on thermal and mass balances. In addition, the condensation debit can be computed as a function of water content and tower height. The balances are considered for a given element of volume with a height of  $dz$ . The obtained model consists

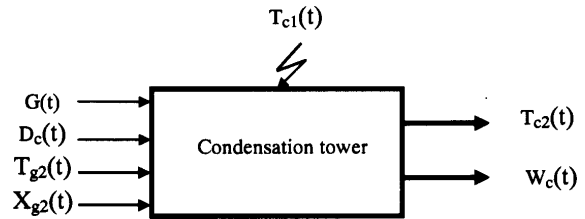


Fig. 4. Input/output diagram of the condensation tower.

of three equations with partial derivatives with respect to time and space, one ordinary differential equation and two algebraic equations using hypotheses listed in [4–11].

- Water phase:

$$m_c C_c \frac{\partial T_c}{\partial t} = -D_c C_c \frac{\partial T_c}{\partial z} + UA(T_{1c} - T_c) \quad (7)$$

- Air phase

$$m_G C_G \frac{\partial T_g}{\partial t} = GC_G \frac{\partial T_g}{\partial z} - h_G A(T_g - T_{1c}) - L_v k_G A(X_G - X_{1c}) \quad (8)$$

and

$$m_G \frac{\partial X_G}{\partial t} = G \frac{\partial X_G}{\partial z} + k_G A(X_G - X_{1c}) \quad (9)$$

$$X_{1c} = X_G + \frac{[h_G(T_g - T_{1c}) + U(T_c - T_{1c})]}{L_v k_G} \quad (10)$$

- Air–condensate interface [7–10]:

$$X_{1c} = 0.62198 \frac{P_I}{1 - P_I}$$

where  $m_G = \epsilon_G \rho_G$ ,  $m_c = \epsilon_c \rho_c$ , and  $P_l$  is the saturation pressure.

Following the water balance  $dW_c = GdX_G$ , the flow rate of the condensed water is:

$$dW_c = k_G A (X_{Ic} - X_G) dz \tag{12}$$

Here, the process of condensation is slow enough to assume that  $dW_c$  can be that at the steady-state condition. The expressions for  $h_G$ ,  $K_G$ ,  $h_e$ ,  $U$ , and  $h_c$  are given in [2].

### 3. Simulation

The operation of desalination by solar energy is extremely sensitive to meteorological variations. Therefore, it was recommended to study the operation of each section of the unit in the presence of such variations. The steady-state simulation revealed the impact of different command signals on the output signals of each unit section [2], while the dynamic model simulation results helped to predict the behaviour of each section as a function of the internal signals variations and the meteorological variations.

#### 3.1. Solar collector

Several simulations of the solar collector dynamic model were made using the dynamic model developed above. The results for solar insolation, fluid temperature at the collector entrance and fluid debit variations on the solar collector outlet temperature are summarized in Table 1.

#### 3.2. Evaporation tower

The parametric study of the evaporation tower using numerical simulation was carried out to study the influence of fluctuations in the water temperature ( $T_{12}$ ) at the tower entrance, variation in the air temperature ( $T_{g1}$ ) at the entrance of the tower, and perturbation in the water and air flow rates ( $L, G$ ) on the output signals ( $T_{g2}, X_{g2}$ ). Results are shown in Table 2.

#### 3.3. Condensation tower

The main objective of the parametric study and numerical simulation of the condensation tower operation was to predict the dynamic behaviour of the tower following external perturbations caused by meteorological

Table 1  
Solar collector simulation results

	Case 1	Case 2	Case 3
$T_{fe}(t)$	Constant	Variable	Constant
$m_f(t)$	Constant	Constant	Variable
$I(t)$	Variable	Constant	Constant
$T_a(t)$	Constant	Constant	Constant
Operating conditions	$T_a = 15^\circ\text{C}$ ; $T_{fe} = 10^\circ\text{C}$ $m_f = 0.02 \text{ l s}^{-1}$	$T_a = 15^\circ\text{C}$ ; $m_f = 0.02 \text{ l s}^{-1}$ $I = 800 \text{ W m}^{-2}$	$T_a = 15^\circ\text{C}$ ; $T_{fe} = 10^\circ\text{C}$ $I = 800 \text{ W m}^{-2}$
$T_{fs}(t)$	Increases with $I$	Increases with $T_{fe}$	Decreases with $m_f$
Notes	100% rise in $I(t)$ yields a 43% increase in $T_{fs}(t)$	Low values of $T_{fe}$ yield high values of $T_{fs}$ High efficiency requires low $T_{fe}$ values	As $m_f$ increases, $T_{fs}$ decreases

Table 2  
Evaporation tower simulation results

	Case 1	Case 2	Case 3	Case 4
$G(t)$	Constant	Constant	Constant	Variable
$L(t)$	Constant	Constant	Variable	Constant
$T_{12}(t)$	Variable	Constant	Constant	Constant
$T_{g1}(t)$	Constant	Variable	Constant	Constant
$X_{g1}(t)$	Constant	Constant	Constant	Constant
Operating conditions:	$T_{g1} = 25^\circ\text{C}$ $X_{g1} = 0.01988$ $t \leq 20$ mn, $T_{12} = 50^\circ\text{C}$ $t > 20$ mn, $T_{12} = 60^\circ\text{C}$	$T_{12} = 50^\circ\text{C}$ , $G = 0.3$ kg s <sup>-1</sup> $L = 0.18$ kg s <sup>-1</sup> , $t \leq 20$ mn, $T_{g1} = 25^\circ\text{C}$ , $X_{g1} = 0.01988$ $t > 20$ mn, $T_{g1} = 35^\circ\text{C}$ , $X_{g1} = 0.03619$	$T_{12} = 50^\circ\text{C}$ , $T_{g1} = 25^\circ\text{C}$ $X_{g1} = 0.01988$ $t \leq 20$ mn, $L = 0.18$ k s <sup>-1</sup> $t > 20$ mn, $L = 0.36$ kg s <sup>-1</sup>	$T_{12} = 50^\circ\text{C}$ , $T_{g1} = 25^\circ\text{C}$ $X_{g1} = 0.01988$ $L = 0.36$ kg s <sup>-1</sup> $t \leq 20$ mn, $G = 0.3$ kg s <sup>-1</sup> $t > 20$ mn, $G = 0.45$ kg s <sup>-1</sup>
$T_{g2}(t)$	Increases with $T_{12}$	Increases with $T_{g1}$	Increases with $L$	Decreases with $G$
$X_{g2}(t)$	Increases with $T_{12}$	Increases with $T_{g1}$	Increases with $L$	Decreases with $G$
Notes:	Similar dynamic response for $T_{g2}$ and $X_{g2}$	A 40% rise in $T_{g1}$ yields an increase of 11% in $T_{g2}$ and 23% in $X_{g2}$ ; $T_{12}$ has more impact on $T_{g2}$ and $X_{g2}$ than $T_{g1}$ does	100% rise in water debit improves $T_{g2}$ by 6% and $X_{g2}$ by 13.15%	A 50% increase in $G$ reduces $T_{g2}$ by 8% and $X_{g2}$ by 15%; Recommended to work with low air debit for best production

conditions and internal perturbations generated by the solar collector and the evaporation tower. To investigate the influence of input signals of the condensation tower —  $G$ ,  $T_{g2}$ ,  $X_{g2}$ ,  $D_c$  and the external perturbations  $T_{c1}$  — on the amount of condensate  $W_c$ , the following series of numerical simulations was carried out using the reduced dynamic model:

- a perturbation of the humid air temperature at the tower top entrance
- a variation in the cooling water debit at the tower lower entrance
- a fluctuation in the cooling water temperature
- a variation in the humid air debit at the top of the tower.

The results are shown in Table 3.

#### 4. Conclusions

As the operation of this type of desalination installation is very sensitive not only to variations of its input signals but also to meteorological condition perturbations, the mathematical modeling of the solar collector, the evaporation and condensation towers in the dynamic mode of operation obtained the best knowledge of the real process and the spatial distribution as well as the time evolution of the unit parameters.

The parametric study carried out using the dynamic simulation of the solar collector was interesting. First, the fluid temperature at the collector exit increased with the solar flux and the fluid temperature at the entrance and second, the fluid temperature at the collector exit decreased as the fluid debit increased. Therefore, it would be recommended to work with a low

Table 3  
Condensation tower simulation results

	Case 1	Case 2	Case 3	Case 4
$G(t)$	Constant	Constant	Constant	Variable
$D_c(t)$	Constant	Constant	Variable	Constant
$T_{g2}(t)$	Variable	Constant	Constant	Constant
$X_{g2}(t)$	Constant	Constant	Constant	Constant
$T_{c1}(t)$	Constant	Variable	Constant	Constant
Operating conditions	$T_{c1}=25^\circ\text{C}$ , $D_c=0.2\text{ kg s}^{-1}$ $G = 0.3\text{ kg s}^{-1}$ $t \leq 20\text{ mn}$ , $T_{G2} = 32^\circ\text{C}$ $X_{G2} = 0.030645$ $t > 20\text{ mn}$ , $T_{G2} = 45^\circ\text{C}$ $X_{G2} = 0.06433$	$G=0.3\text{ kg s}^{-1}$ , $T_{c1}=25^\circ\text{C}$ $T_{G2} = 32^\circ\text{C}$ $X_{G2} = 0.030645$ $t \leq 20\text{ mn}$ , $D_c = 0.2\text{ kg s}^{-1}$ $t > 20\text{ mn}$ , $D_c = 0.4\text{ kg s}^{-1}$	$D_c = 0.2\text{ kg s}^{-1}$ $G = 0.3\text{ kg s}^{-1}$ $T_{G2} = 32^\circ\text{C}$ $X_{G2} = 0.030645$ $t \leq 20\text{ mn}$ , $T_{c1} = 25^\circ\text{C}$ $t > 20\text{ mn}$ , $T_{c1} = 15^\circ\text{C}$	$D_c = 0.2\text{ kg s}^{-1}$ $T_{c1} = 25^\circ\text{C}$ $T_{G2} = 32^\circ\text{C}$ $X_{G2} = 0.030645$ $t \leq 20\text{ mn}$ , $G = 0.3\text{ kg s}^{-1}$ $t > 20\text{ mn}$ , $G = 0.15\text{ kg s}^{-1}$
$T_{c2}(t)$	Increases with $T_{g2}$	No change	Decreases $D_c$	Increases with $G$
$W_c(t)$	Increases with $T_{g2}$	No change	Decreases $D_c$	Increases with $G$
Notes:	$W_c$ is sensitive to $T_{g2}$ . A 40% rise in $T_{g2}$ increased $W_c$ by 264.5% (3.75 kg/h)		40 % reduction in cooling water temperature improved $W_c$ by 69.87%; Use low cooling temperature for best production	50% variation in $G$ produced 21.75% variation in $W_c$ ; $G$ has more impact on $W_c$ than $T_{g2}$

water debit so as to have the highest possible temperature at the collector outlet.

The optimal operation of the evaporation tower requires also a significant water debit, a high water temperature, and finally a minimum air debit at the entrance level. Therefore, the following compromises should be made:

- the use of storage tank permitting the fluid circulation in a closed circuit between the solar collectors and the tank. This solution has the advantage of increasing water temperature and enabling the operation with a relatively high water debit. However, it creates a discontinuity in the process since during the operation in a closed circuit, water does not enter the evaporation tower;
- the use of multiple solar collectors connected in series and parallel combinations to insure a

very high water temperature due to the series set-up and a high water debit due to the parallel set-up;

- the use of recycling technique. This would reclaim the amount of hot water that did not evaporate from the bottom of the evaporation tower and mix it with the hot water coming from the solar collector before injection into the evaporation tower. This technique would increase the water debit but with a limited temperature improvement.
- Operation with a low air debit in the tower guarantees a high temperature at the tower exit with a significant water content.

Following this study, it can be concluded that the optimal operation of the condensation tower requires at the entrance level a high humid air



## References

- [1] A. Bohner, Desalination, 73 (1989) 197.
- [2] H. Ben Bacha, A.Y. Maalej, H. Ben Dhia, I. Ulber, H. Uchtmann, M. Engelhardt and J. Krelle, Desalination, 122 (1999) 177.
- [3] R. Gicquel, Revue général de thermique, 184 (1977) 327.
- [4] H. Ben Bacha, Modélisation et simulation en vue de la commande d'une unité de dessalement d'eau par l'énergie solaire, Thèse de doctorat de spécialité en Génie Electrique (automatique), ESSTT, Tunis, 1996.
- [5] MA. Younis, M.A. Fahim and N. Wakao, J. Chem. Engineering Jpn., 20 (1987) 614.
- [6] S. Kaguel, M. Nishio and N. Wakao, Internat. J. Heat Mass Transf., 31 (1988) 2579.
- [7] R. Cretinon, Tech. l'Ingénieur, R 3045 (1995) 1.
- [8] D. Sonntag, Z. Meteorologie, 70 (1990) 5/340.
- [9] A. Wexler, J. Res. Nat. Bureau Standards A., Physics and Chemistry, 80A (1976) 775.
- [10] A. Wexler, J. Res. Nat. Bureau Standards A., Physics and Chemistry, 81A (1977) 5.
- [11] A. Grehier and A. Rojey, Revue l'Institut Français Pétrole, 1 (1989) 77.